Heme oxygenase 1-overexpressing bone marrow mesenchymal stem cell-derived exosomes suppress interleukin-1 beta-induced apoptosis and aging of nucleus pulposus cells

HAO ZHANG[1*], DI ZHANG[1*], HUI WANG[1], YILEI LIU[1], WENYUAN DING[1], GUANGPU FAN[2] and XIANZHONG MENG[3]

[1]Spinal Surgery Department 2, Hebei Medical University Third Hospital, Shijiazhuang, Hebei 050011, P.R. China; [2]Department of Cardiac Surgery, Peking University People's Hospital, Beijing 100044, P.R. China; [3]Spinal Surgery Department 1, Hebei Medical University Third Hospital, Shijiazhuang, Hebei 050011, P.R. China

Received September 23, 2024; Accepted February 13, 2025

DOI: 10.3892/mmr.2025.13481

Abstract. Exosomes derived from bone marrow mesenchymal stem cells (BMSCs) and heme oxygenase 1 (HO-1) attenuate intervertebral disc degeneration (IVDD). However, whether BMSC-derived exosomes attenuate IVDD by delivering HO-1 to nucleus pulposus (NP) cells remains to be elucidated. Mouse BMSCs were characterized by multilineage differentiation and surface marker molecule detection. Exosomes Exo and Exo-HO-1 were isolated from BMSCs and HO-1-overexpressing BMSCs by ultracentrifugation and characterized by observing their morphology, detecting the exosome marker proteins, tumor susceptibility gene 101 (TSG101) and CD63 and analyzing their particle size. Interleukin-1 β (IL-1β)-stimulated NP cells were used as the IVDD cell model. The influence of Exo or Exo-HO-1 on IL-1β-urged apoptosis and senescence in NP cells was determined by flow cytometry, western blotting and senescence-associated β-galactosidase (SA-β-gal) staining. Exo and Exo-HO-1 did not vary in size or morphology. Exo-HO-1 markedly repressed IL-1β-prompted apoptosis in NP cells, accompanied with a prominent increase in Cleaved caspase 3 and Bax protein levels and a marked decrease in Bcl-2 protein levels. Exo and Exo-HO-1 both decreased the number of SA-β-gal-positive NP cells and arrested NP cells in the G_1 phase. Exo-HO-1 had stronger effects than Exo, suggesting that Exo-HO-1 can weaken IL-1β-induced NP cell senescence. In addition, Exo and Exo-HO-1 repressed IL-1β mediating the phosphorylation of p65 and nuclear translocation of p65. In conclusion, HO-1-overexpressing BMSC-derived exosomes blocked the nuclear factor-kappa B signaling in IL-1β-stimulated NP cells, thus impairing cell apoptosis and senescence.

Correspondence to: Dr Xianzhong Meng, Spinal Surgery Department 1, Hebei Medical University Third Hospital, 139 Ziqiang Road, Qiaoxi, Shijiazhuang, Hebei 050011, P.R. China
E-mail: 36700973@hebmu.edu.cn

*Contributed equally

Key words: mesenchymal stem cells, heme oxygenase 1, exosomes, nucleus pulposus

Introduction

Chronic low back pain due to intervertebral disc (IVD) degeneration (IVDD) is a ubiquitous disease that seriously affects the quality of life of patients and causes heavy social and economic burdens (1). Around 619 million individuals globally had low back pain in 2020 (accounting for nearly 10% of the world population) and this number is estimated to reach 843 million by 2050 (2). The prevalence of IVDD in the elderly is high at 90% (3). IVDD is mainly caused by the accumulation of interleukin (IL)-1 beta (IL-1β), loss of proteoglycans and diffusion of cytokines into the extracellular matrix, leading to activation of MMPs, eventually contributing to the pathologic apoptosis of nucleus pulposus (NP) cells (4,5). Currently, clinical treatments for IVDD are mainly conservative treatment and surgery, which can relieve symptoms and reduce pain, but cannot reverse IVDD (6). Therefore, seeking therapeutic measures to delay IVDD progression or even reverse the IVDD process has become a hot topic in current research.

Mesenchymal stem cell (MSC) therapy for IVDD has received extensive attention (7). IVD cannot provide adequate nutrition for transplanted MSCs because of the lack of vascular structures (8). In addition, the death of transplanted MSCs releases deleterious substances, thereby exacerbating IVDD (9). Exosomes produced by MSCs through paracrine secretion retain the potential of MSCs and act as carriers to deliver their contents (metabolites, amino acids, lipids, proteins and nucleic acids) to target cells to modulate their activity. Exosomes have a diameter of 30-200 nm (10). Xiao *et al* (11) revealed that bone mesenchymal stem cell (BMSC)-derived exosomes weaken NP cell autophagy by regulating the protein kinase B/mammalian target of rapamycin pathway. Additionally, BMSC-derived exosomes can improve IVDD by modulating macrophage polarization through the delivery of hypermethylated lncRNAs in colorectal adenocarcinoma (12). Due to their

low immunogenicity, good compatibility and avoidance of the adverse effects of MSC therapy, MSC-derived exosomes are considered emerging therapeutic methods for IVDD (13,14). Studies have demonstrated that the clinical efficacy of exosomes can be improved by altering their composition. For instance, Netrin1-enriched exosomes from genetically modified adipose-derived stem cells protect muscles, reduce inflammation, improve collateral artery remodeling and enhance angiogenesis, thereby improving diabetic limb ischemia (15). In addition, exosomes derived from BMSCs modified with miR-340-3p inhibited ferroptosis to facilitate the recovery of the injured rat uterus (16). Therefore, exosomes modified with specific genes may provide additional strategies for the treatment of IVDD.

Heme oxygenase 1 (HO-1) protein is encoded by HMOX1, which catalyzes the degradation of heme and production of bilirubin, carbon monoxide and ferrous ions (Fe^{2+}) (17). HO-1 is associated with various diseases including osteoarthritis (18), diabetes (19) and cancer (20). In addition, MSC-derived exosomes have been revealed to weaken the process of diverse diseases, such as delayed neurocognitive recovery (21), spinal cord injury (22) and acute liver injury (23) by mediating HO-1 expression. In addition, HO-1 exerts a protective role in the process of IVDD (24,25). However, whether HO-1-enriched BMSC-derived exosomes play a protective role in IVDD remains unclear.

Although both BMSC-derived exosomes and HO-1 have been demonstrated to exert protective effects against IVDD progression, the efficacy of HO-1-modified BMSC-derived exosomes remains unclear. Thus, the present study aimed to investigate the effects of exosomes derived from HO-1-overexpressing BMSCs on the apoptosis and senescence of IL-1β-stimulated NP cells, offering evidence to support the clinical utilization of HO-1-modified BMSC-derived exosomes in IVDD.

Materials and methods

Incubation of BMSCs, NP and 293T cells. Mouse BMSCs [CP-M131 (https://www.procell.com.cn/view/2537.html), Procell Life Science & Technology Co., Ltd.] and NP cells [CP-M146 (https://www.procell.com.cn/view/2549.html), Procell Life Science & Technology Co., Ltd.], two non-immortalized populations, were cultured in Dulbecco's modified Eagle's medium (DMEM; MilliporeSigma) supplemented with 10% fetal bovine serum (Thermo Fisher Scientific, Inc.) and 1% penicillin/streptomycin (Procell Life Science & Technology Co., Ltd.) at 37˚C with additional 5% CO_2. BMSCs and NP cells from passages 2-5 were used. 293T cells (cat. no. CL-0005 Procell Life Science & Technology Co., Ltd.) were also cultured in DMEM with 10% FBS and 1% penicillin/streptomycin in an incubator at 37˚C and 5% CO_2. Ethical approval was waived because the present study did not involve human or animal subjects.

Multilineage differentiation of BMSCs. The potential of mouse BMSCs for multilineage differentiation was analyzed using osteogenic, lipogenic and chondrogenic differentiation assays. Mouse BMSCs were incubated for 2 or 3 weeks in an osteogenic/adipogenic/chondrogenic-induced differentiation medium (Procell Life Science & Technology Co., Ltd.). Finally, mineralized nodules were characterized by alizarin red staining (ARS), lipid droplets were visualized by oil red O (ORO) staining and acidic polysaccharides were characterized by alizarin blue (ALB) staining. For ARS, the incubated BMSCs were fixed in 4% paraformaldehyde (PFA) for 15 min at room temperature. After washing with phosphate-buffered saline (PBS), the cells were stained with ARS solution (40 mM; cat. no. S0141; Cyagen Biosciences, Inc.) for 5 min at room temperature (26). For ORO staining, BMSCs were fixed with 4% PFA for 20 min at room temperature. After soaking in 70% ethanol (cat. no. ml094574; Mlbio Biosciences, Inc.) for 30 sec at room temperature, the cells were stained with ORO working solution (0.5 ml; cat. no. MUXMX-90031, Cyagen Biosciences, Inc.) for 30 min at room temperature and stopped by washing with PBS (27). For ALB staining, BMSCs were stabilized with 4% PFA for 15 min at room temperature and stained with BCIP/NBT working solution (0.5 ml; cat. no. C3206; Beyotime Institute of Biotechnology) away from light for 15 min at 37˚C (28). Images of all stained sections were captured successfully using an inverted microscope (Olympus Corporation).

Identification of BMSCs by flow cytometry. BMSCs were re-suspended and aliquoted into EP tubes (100 µl/tube). BMSCs were incubated with CD29 (5 µl; cat. no. E-AB-F1309D, Wuhan Elabscience Biotechnology Co., Ltd.), CD73 (5 µl; cat. no. E-AB-F1089D, Wuhan Elabscience Biotechnology Co., Ltd.), CD90 (5 µl; cat. no. E-AB-F1283D, Wuhan Elabscience Biotechnology Co., Ltd.), CD34 (5 µl; cat. no. E-AB-F1284D, Wuhan Elabscience Biotechnology Co., Ltd.) and CD45 (5 µl; cat. no. E-AB-F1136D, Wuhan Elabscience Biotechnology Co., Ltd.) antibodies for 30 min at 4˚C in the dark. BMSCs were treated with a mouse anti-immunoglobulin G antibody in a separate tube as a negative control. Following incubation, cells were detected with a FACSCalibur flow cytometer (BD Biosciences) and the data were analyzed with FlowJo software version 10.8.1 (FlowJo LLC Biosciences).

Establishment of BMSCs with stable HMOX1 overexpression. The full-length HMOX1 cDNA was inserted into the pHBLV-CMV-MCS-GFP vector (Hanbio Biotechnology Co., Ltd.) to construct the pHBLV-CMV-MCS-GFP-HMOX1 vector. For lentiviral packaging, a second-generation transduction system was used. 293T cells were co-transfected with pHBLV-CMV-MCS-GFP-HMOX1, pHBLV-CMV-MCS-GFP), pSPAX2 (cat. no. 12260; Addgene, Inc.), and pMD2G (cat. no. 12259; Addgene, Inc.) plasmids at 2:2:1 ratio (10 µg : 10 µg : 5 µg, respectively) using the Simple-fect reagent (Signaling Dawn Biotech) following the manufacturer's instructions. After 48 h, lentivirus particles from the medium were collected by centrifugation (800 x g, 10 min, 4˚C) and filtered via a 0.45-µm filter, and BMSCs were plated at a density of $1x10^5$ cells in 3.5-mm dishes with negative lentiviral particles or HMOX1-overexpressing lentiviral particles (multiplicity of infection=20). At 24 h later, BMSCs were selected with 1 µg/ml puromycin for 3 days prior to subsequent experiments.

Isolation and identification of exosomes from BMSCs. Exosomes isolated from BMSCs with and without HO-1 overexpression were named Exo and Exo-HO-1, respectively.

Briefly, the medium was changed to serum-free DMEM and the cells were incubated for 24 h at 37˚C. To remove dead cells and cell debris, cell supernatants were centrifuged for 10 min (300 x g), 10 min (2,000 x g), and 30 min (10,000 x g) at 4˚C (29). The supernatants were subsequently centrifuged (200,000 x g, 70 min, 4˚C) twice to obtain exosomes. The morphology of the precipitated exosomes was observed using transmission electron microscopy (TEM; JEOL, Ltd.). Determination of exosome-specific markers (TGS101 and CD63) and the endoplasmic reticulum marker cainexin was performed by western blotting without loading control blots in accordance with published references (30-32). The size distribution of Exo and Exo-HO-1 was determined by nanoparticle tracking analysis (NTA) using a ZetaView PMX 110 (Particle Metrix).

Exosome labeling and tracking. The exosomes were labeled with green fluorescent PKH67 (cat. no. 40781; Shanghai Yeasen Biotechnology Co., Ltd.). Briefly, the amount of exosomal protein was determined using the bicinchoninic acid (BCA) protein assay kit (CoWin Biosciences). Dilution buffer was used to prepare the PKH6 dye working solution at a concentration of 100 μM. The exosomes (20 μg) were added 50 μl of the dye working solution and vortexed for 1 min at room temperature. After 10 min of incubation at room temperature, the exosomes were washed and centrifuged (12,000 x g, 2 min, 4˚C) to remove excess PKH67. Labeled exosomes were co-cultured with NP cells for 24 h at 37˚C and then fixed with 4% paraformaldehyde for 20 min at room temperature. After staining with 4',6-diamidino-2-phenylindole, the uptake of labeled exosomes by NP cells was observed using a confocal microscope (Leica Microsystems GmbH).

NP cell treatment. To simulate the pathological environment of IVDD *in vitro*, healthy NP cells ($2x10^5$ cells/well) reaching 70-80% were treated with different concentrations of IL-1β (0, 5, 10 and 20 ng/ml; Shanghai Yeasen Biotechnology Co., Ltd.) for 24 h and a concentration of 10 ng/ml IL-1β was utilized to stimulate NP cells for different times (0, 12, 24 and 48 h) at 37˚C (33,34). To screen for the optimal therapeutic dose of Exo-HO-1, the cells ($2x10^5$ cells/well) were incubated with different concentrations of Exo-HO-1 (0, 10, 20 and 40 μg) in the absence or presence of IL-1β (10 ng/ml) for 24 h at 37˚C. NP cells were incubated in the presence of both IL-1β (10 ng/ml) and Exo-HO-1 (20 μg) for different times (0, 12, 24, 48 and 72 h) at 37˚C (35). NP cells were stimulated with 10 ng/ml of IL-1β and treated with Exo-HO-1 at 37˚C in the meantime and the medium was replaced with fresh medium containing Exo-HO-1 without IL-1β 24 h later. After incubation, the NP cells were used for experimental analysis.

Cell apoptosis analysis. Briefly, different groups of NP cells were harvested using 0.25% trypsin (Procell Life Science & Technology Co., Ltd.), washed twice with PBS and centrifuged (300 x g) for 5 min at 4˚C. The cells were resuspended in 1X binding buffer. Cell apoptosis was determined using an apoptosis kit (Beijing Solarbio Science & Technology Co., Ltd.), according to the manufacturer's instructions. Cells (~$5x10^5$) were incubated with 5 μl of Annexin V/FITC in a flow tube (5 ml) for 5 min under light protection at room temperature. Finally, 5 μl of propidium iodide solution was added and incubated for 5 min at room temperature. A FACSCalibur flow cytometer was used to analyze the cells immediately. The collected data were analyzed using FlowJo software version 10.8.1 (FlowJo LLC Biosciences). The apoptosis rate is the sum of early apoptotic cells and the percentage of late apoptotic cells.

Cell viability analysis. After incubation of NP cells with the different treatments, 10 μl of the Cell Counting Kit-8 (CCK-8; Beijing Solarbio Science & Technology Co., Ltd.) reagent was added into each well. After incubation for 2 h, the absorbance was measured at 450 nm using a plate reader (Thermo Fisher Scientific, Inc.).

Cell cycle analysis. The collected NP cells were fixed in 70% ethanol (1 ml) at 4˚C overnight. After washing and centrifugation (1,000 x g; 3 min, 4˚C), the NP cells were incubated with a mixture of staining solution containing the staining buffer (500 μl), propidium iodide staining solution (X20; 25 μl) and RNase A (20x; 10 μl) at room temperature for 30 min in the dark. These reagents were included in the Cell Cycle and Apoptosis Detection Kit (cat. no. C1052; Beyotime Institute of Biotechnology). The stained cells were analyzed using flow cytometry (BD Biosciences) at an excitation wavelength of 488 nm and an emission wavelength of 605 nm.

Subcellular fractionation. Nuclear and cytoplasmic components were separated using a Nuclear and Cytoplasmic Protein Extraction Kit (cat. no. P0028; Beyotime Institute of Biotechnology). In brief, NP cells were digested with cytoplasmic protein extraction reagent A supplemented with PMSF on ice for 15 min. Subsequently, 10 μl of the reagent B was added and vortexed vigorously for 5 sec, followed by incubation on ice for 1 min. Centrifugation was performed for 5 min (4˚C; 12,000 x g) after another vortex for 5 sec and the obtained supernatants were cytoplasmic proteins. After aspirating the supernatant, 50 μl of PMSF-supplemented nuclear protein extraction reagent was added to the precipitate. After vigorous vortex for 20 sec, the samples were placed on ice for 30 min, with high-speed vortex every 1-2 min for 20 sec. Supernatants harvested by centrifugation (4˚C; 12,000 x g) were cytoplasmic proteins.

Western blotting. Radioimmunoprecipitation analysis lysis buffer (Beijing Solarbio Science & Technology Co., Ltd.) was used to extract proteins from NP cells and exosomes. For protein quantification, a BCA protein assay kit (CoWin Biosciences) was used according to the manufacturer's instructions. The extracted protein samples (30 μg) were electrophoresed by 8-12% sodium dodecyl sulfate-polyacrylamide gel electrophoresis and transferred onto polyvinylidene difluoride membranes (MilliporeSigma). After blocking with a rapid blocking solution (Beyotime Institute of Biotechnology) at 4˚C overnight, the membranes were incubated with appropriate primary antibodies including anti-HO-1 (cat. no. GTX637432; 1:2,000; GeneTex, Inc.), anti-TGS101 (cat. no. A01233-2, 0.25 μg/ml; Boster Bio), anti-CD63 (FNab01490; 1:1,000; Fine Biotech Co., Ltd, Wuhan, China) and anti-Cainexin (cat. no. GTX109669; 1:5,000; GeneTex, Inc.), Bcl-2 (cat. no. FNab00839; 1:1,000; Wuhan Fine Biotech Co., Ltd.), Bax (cat. no. FNab00810;

1:2,000; Wuhan Fine Biotech Co., Ltd.), cleaved caspase 3 (cat. no. MBS9410752; 1:1,000; MyBioSource, Inc.), anti-p65 (cat. no. PB9324; 0.5 μg/ml; Boster Bio), anti-p-p65 (cat. no. A00284S468-2; 1:2,000; Boster Bio), anti-GAPDH (cat. no. H00227; 1:5,000; Boster Bio) and anti-Histone H3 (cat. no. M12477-9; 1:1,000; Boster Bio) antibodies. After incubation with goat anti-rabbit IgG-HRP secondary antibody (cat. no. GTX213110-01; 1:5,000; GeneTex, Inc.) for 2 h at room temperature, an enhanced chemiluminescence reagent (cat. no. P0018; Beyotime Institute of Biotechnology) was used to visualize the results. Band intensity was quantified using the ImageJ software (version v1.48; National Institutes of Health).

Senescence-associated β-galactosidase (SA-β-gal) staining. SA-β-gal-positive NP cells were quantified using the SA-β-gal staining kit (cat. no. C0602; Beyotime Institute of Biotechnology). After incubation, NP cells in 6-well plates were fixed for 15 min using a fixation solution (1 ml) included in the kit. After rinsing twice with PBS, the cells were stained with the SA-β-gal staining solution (1 ml) overnight at 37˚C. Following rinsing, SA-β-gal-positive NP cells were observed under an inverted microscope (Olympus Corporation).

Statistical analysis. A minimum of three biological replicates were used in all the experiments. Statistical significance was assessed using the GraphPad Prism 8 software (GraphPad; Dotmatics). Continuous data are expressed as means ± standard errors of the mean. Normality of the data was assessed using the Shapiro-Wilk test. Differences between two groups were analyzed using unpaired t-tests and one-way analysis of variance followed by Tukey's post hoc test was performed for multiple-group differences. $P<0.05$ was considered to indicate a statistically significant difference.

Results

Incubation and characterization of BMSCs. To elucidate the mechanism underlying the protective effect of BMSCs against NP cells during IVDD, the present study first determined the multilineage differentiation capacity of the purchased BMSCs. Growth and morphological changes in cultured primary BMSCs were observed using an inverted microscope. BMSCs were distributed uniformly and showed a spindle-like morphology (Fig. 1A). After 14 days of incubation with the osteogenic culture medium for BMSCs, ARS showed distinct mineralized nodule formation (Fig. 1A). After induction with lipogenic medium, ORO staining showed evident fat droplet formation, indicating the differentiation of BMSCs into adipocytes (Fig. 1A). Alcian blue staining showed a marked accumulation of glycosaminoglycans following incubation in chondrogenic medium (Fig. 1A). Flow cytometry for stem cell surface antigens showed that they were highly positive surface markers CD29 (99.96%), CD73 (99.50%) and CD90 (94.33%), accompanied by negative surface markers CD34 (1.08%) and CD45 (2.44%). The multidirectional differentiation potential and highly positive surface markers suggested high purity of the cultured BMSCs.

Characterization of Exo and Exo-HO-1. HO-1 protein encoded by the HMOX1 gene possesses a protective effect on NP cells in IVDD (36,37). To characterize the effect of HMOX1-overexpressing BMSC-derived exosomes on IVDD, HMOX1 overexpression plasmids were transfected into BMSCs. A schematic representation of the HMOX1 overexpression plasmid is shown in Fig. 2A. The green fluorescence exhibited by BMSCs after transfection suggested the successful expression of the plasmid DNA (Fig. 2B). HMOX1 mRNA and HO-1 protein levels were markedly upregulated following transfection, as confirmed by RT-qPCR and western blotting, respectively (Fig. 2C and D). Next, exosomes were extracted from the BMSCs transfected with the vector or HMOX1 by ultracentrifugation and termed Exo and Exo-HO-1, respectively. The diameters of both Exo and Exo-HO-1 with cup or spherical shapes were observed to be ~100 nm using TEM (Fig. 2E). The exosome marker proteins tumor susceptibility gene 101 (TSG101) and CD63 were more strongly expressed in Exo and Exo-HO-1 cells than in BMSCs, whereas calnexin (an endoplasmic reticulum protein) was not detected in Exo or Exo-HO-1 cells, indicating that the isolated exosomes were not contaminated with cellular components (Fig. 2F). NTA showed that these particles, which were ~114 nm in diameter, were the most abundant, with most of the particles <200 nm (Fig. 2G). A significant upregulation of HO-1 protein was observed in Exo-HO-1 compared with that in Exo, indicating that Exo-HO-1 carried greater amounts of HO-1 protein (Fig. 2H). The aforementioned analyses showed that Exo and Exo-HO-1 were successfully isolated.

Analysis of optimal conditions for IL-1β incubation and Exo-HO-1 treatment. To investigate the effects of IL-1β treatment on the apoptosis of NP cells, different IL-1β concentrations (0, 5, 10 and 20 ng/ml) were used to stimulate the cells for 24 h. As shown in Fig. 3A, IL-1β (10 and 20 ng/ml) stimulation urged NP cell apoptosis markedly. Next, the NP cells were stimulated with 10 ng/ml for different durations. Apoptosis of the NP cells increased progressively with the prolongation of IL-1β stimulation (Fig. 3B). The apoptosis of NP cells was shifted to a later stage when the concentration of IL-1β reached 20 ng/ml or when 10 ng/ml of IL-1β was treated for 48 h. Consequently, NP cells were stimulated with 10 ng/ml of IL-1β for 24 h to induce IVDD cell models *in vitro*. To evaluate the effects of Exo-HO-1 on NP cell viability, we treated the cells with different doses of Exo-HO-1 (0, 10, 20 and 40 μg) for 24 h in the presence or absence of IL-1β. The results revealed that Exo-HO-1 treatment did not affect the viability of healthy NP cells, whereas Exo-HO-1 treatment improved the viability of NP cells under IL-1β stimulation once the concentration reached 20 μg (Fig. 3C and D). Subsequently, the viability of NP cells treated with Exo-HO-1 (20 μg) at different times (0, 12, 24, 48 and 72 h) was explored. Incubation of IL-1β-induced NP cells with Exo-HO-1 for ≥24 h could improve their activity, so IL-1β-stimulated NP cells treated with Exo-HO-1 (20 μg) for 48 h were used for subsequent analysis (Fig. 3E).

Exo-HO-1 protects NP cells against IL-1β-urged apoptosis. Based on these results, PKH67-labeled Exo or Exo-HO-1 were co-incubated with NP cells to observe the uptake of exosomes by NP cells. As shown in Fig. 4A, PKH67-labeled Exo or Exo-HO-1 were taken up by NP cells (Fig. 4A). In addition, NP cells co-cultured with Exo-HO-1 showed overtly higher HO-1 protein levels than those incubated with Exo (Fig. 4B).

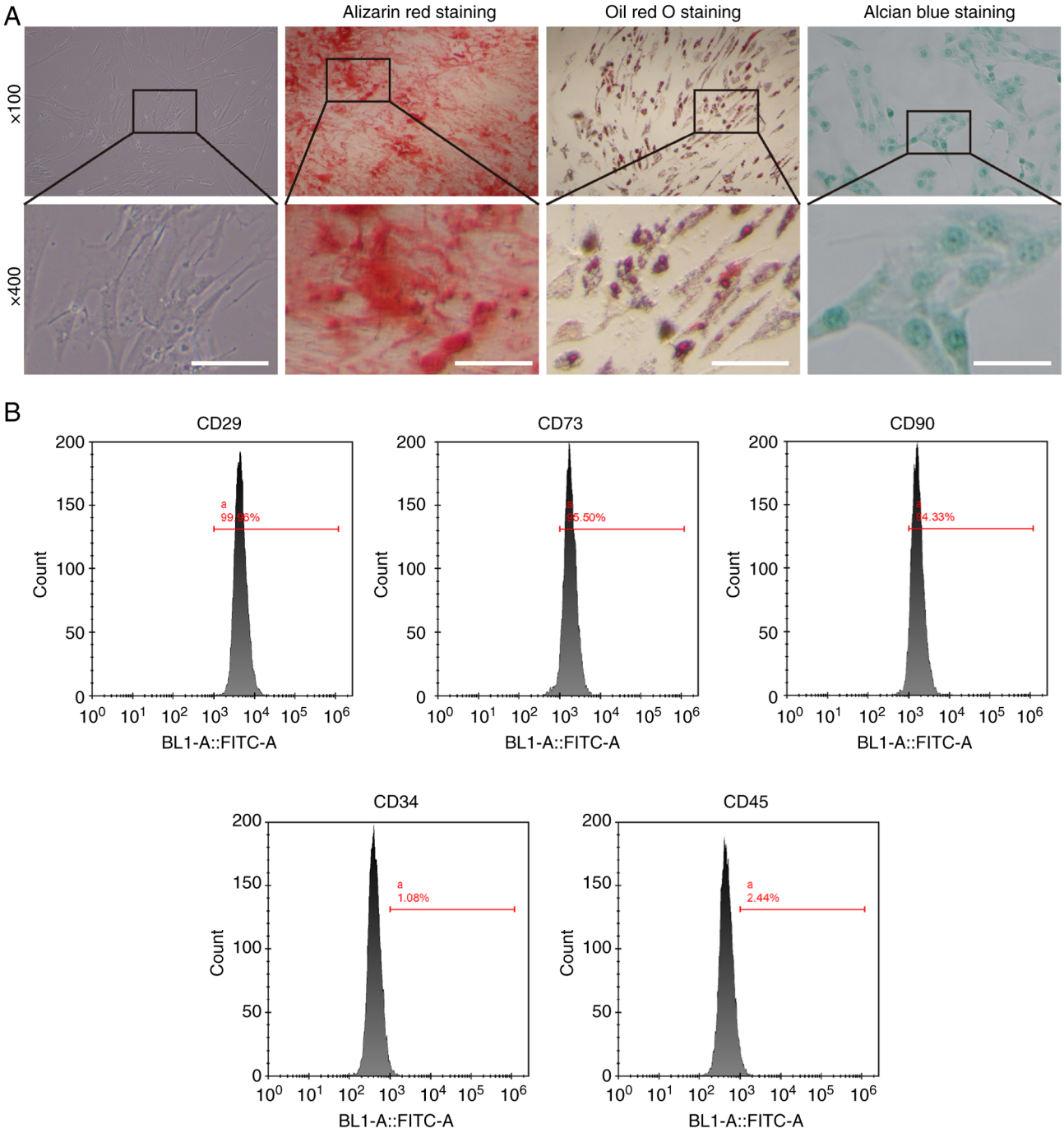

Figure 1. Incubation and characterization of BMSCs. (A) Representative images of BMSCs with spindle-like morphology under the microscope (scale bar, 100 μm). Representative images of alizarin red S staining, oil red O staining and Alcian blue staining of BMSCs differentiated into osteoblasts, adipocytes, or chondrocytes (scale bar, 100 μm). (B) Flow cytometry analysis of BMSCs for cell surface markers CD29, CD73, CD90, CD34 and CD45. BMSCs, bone marrow mesenchymal stem cells.

Flow cytometry was used to evaluate NP cell apoptosis. IL-1β stimulation resulted in marked apoptosis of NP cells, accompanied with a notable reduction in Bcl-2 protein levels and a prominent elevation in Bax and cleaved caspase 3 protein levels. Exo treatment had no effect on NP cell apoptosis under IL-1β stimulation. However, Exo-HO-1 treatment attenuated IL-1β-urged NP cell apoptosis, with synchronized alterations in apoptosis-associated proteins (Fig. 4C and D). Collectively, these results indicated that Exo-HO-1 mitigated NP cell apoptosis under IL-1β stimulation.

Exo-HO-1 impairs IL-1β-prompted NP cell senescence. Subsequently, the effects of Exo-HO-1 on NP cell senescence under IL-1β stimulation were further investigated. The number of SA-β-gal-positive NP cells was markedly elevated after IL-1β stimulation. Although treatment with both Exo and Exo-HO-1 reduced the number of SA-β-gal-positive NP cells in response to IL-1β stimulation, the effect of Exo-HO-1 was stronger than that of Exo (Fig. 5A). Senescence arrest occurs mainly in the G_0/G_1 phase of the cell cycle. Therefore, the aforementioned results were further validated using cell cycle assays. IL-1β

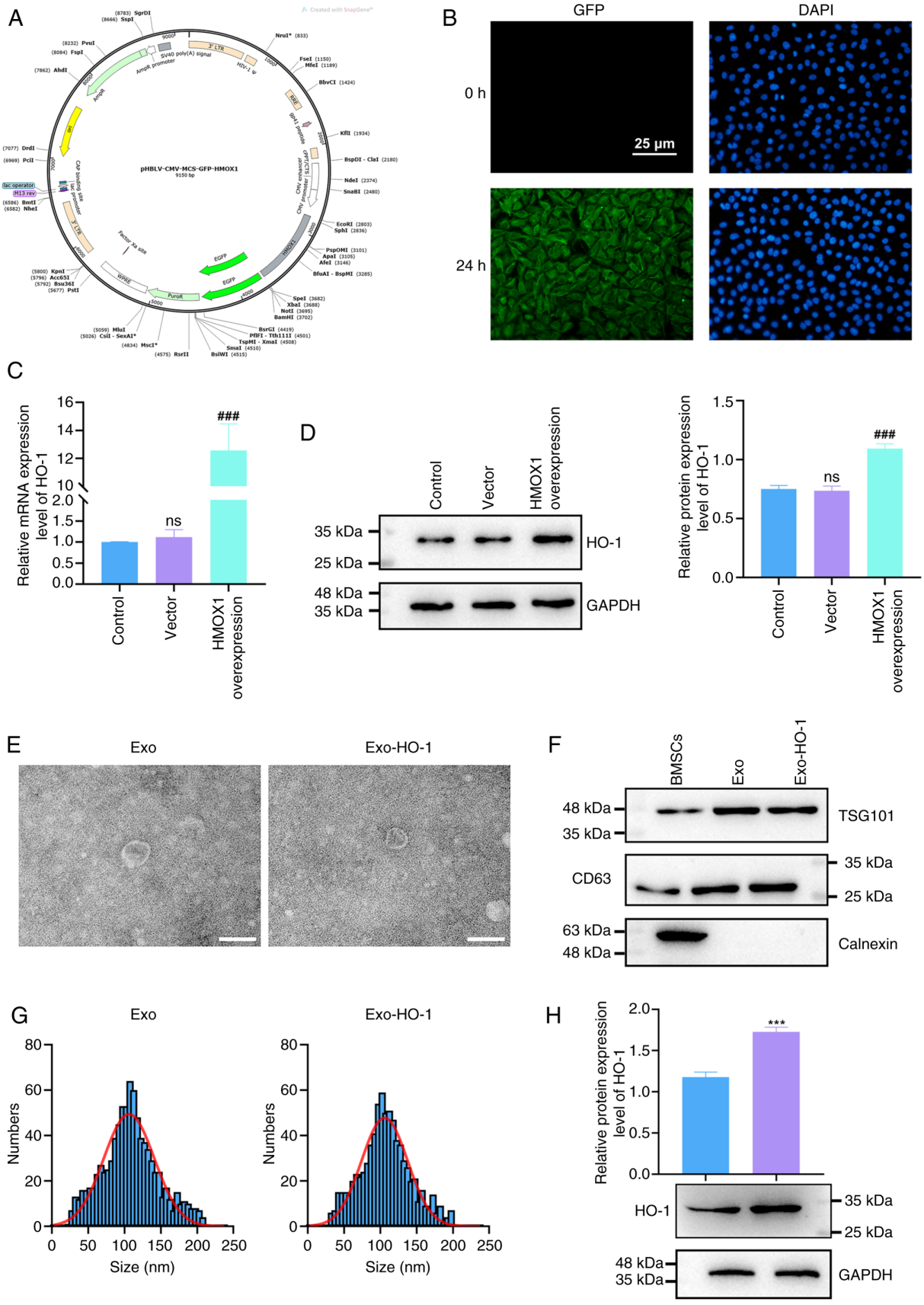

Figure 2. Characterization of Exo and Exo-HO-1. (A) A schematic representation of the HMOX1-overexpressing plasmid. (B) Fluorescent images of BMSCs transfected by the HMOX1-overexpressing plasmid. (C and D) Transfection efficiency of HMOX1 overexpression plasmids was verified by quantitative reverse transcription polymerase chain reaction and western blotting. (E) Morphology of BMSC-derived exosomes Exo and Exo-HO-1 under transmission electron microscopy. Scale bar, 100 nm. (F) Western blotting detected the exosome marker proteins TSG101 and CD63 and the endoplasmic reticulum protein Calnexin in Exo, Exo-HO-1 and BMSCs. (G) Size distribution of BMSC-derived exosomes Exo and Exo-HO-1 was analyzed by nanoparticle tracking analysis. (H) Western blotting evaluated HO-1 protein levels in exosomes Exo and Exo-HO-1. $^{###}$P<0.001 vs. vector; ***P<0.001 vs. Exo; ns, not significant. Exo, exosomes; HO-1, heme oxygenase 1; BMSCs, bone marrow mesenchymal stem cells; TSG101, tumor susceptibility gene 101.

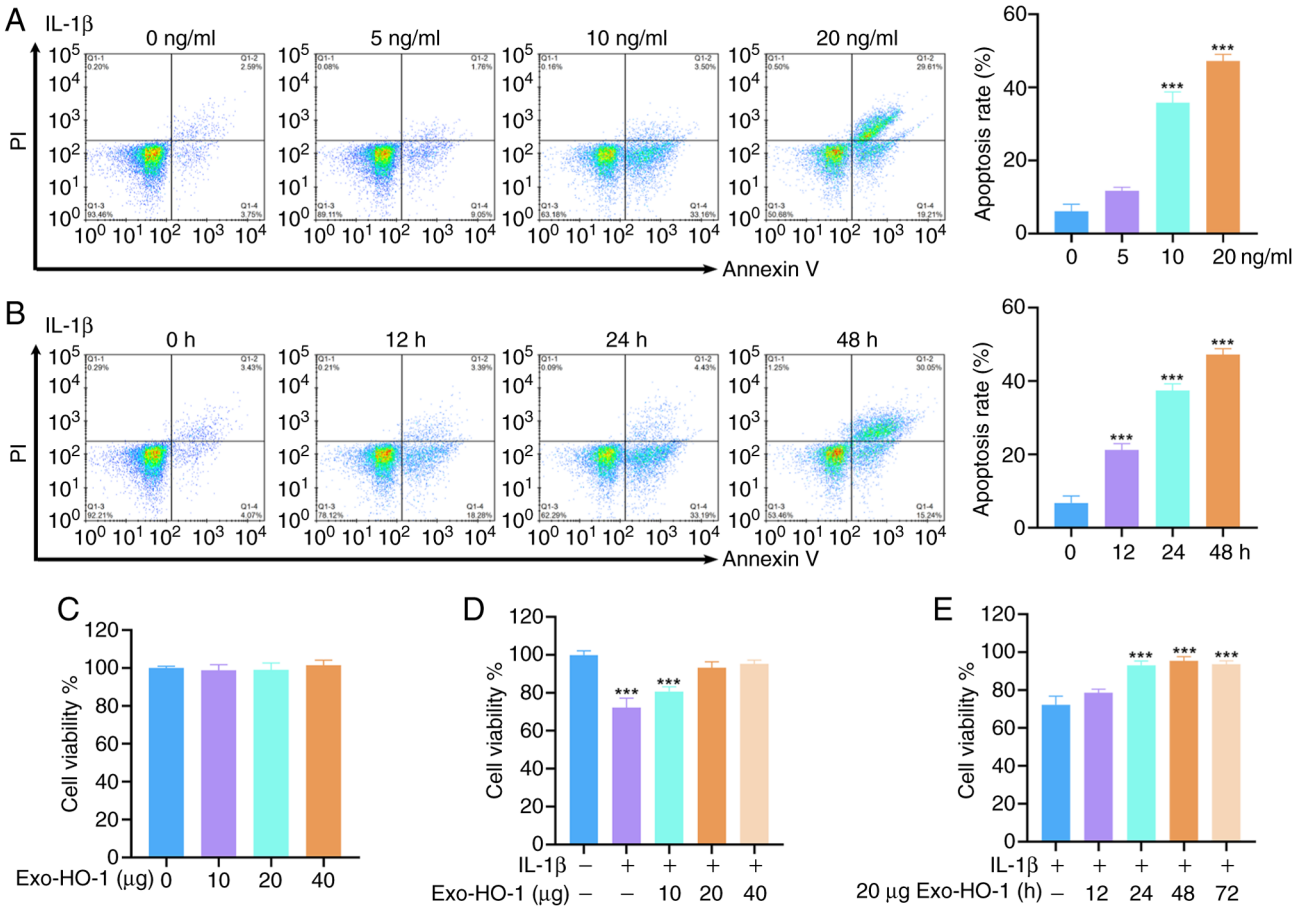

Figure 3. Determination of optimal conditions for IL-1β incubation and Exo-HO-1 treatment. (A and B) NP cells were stimulated with different concentrations of IL-1β (0, 5, 10 and 20 ng/ml) for 24 h or IL-1β (10 ng/ml) for different times (0, 12, 14 and 48 h). The apoptosis of NP cells was determined by flow cytometry. (C and D) NP cells were treated with different doses of Exo-HO-1 (0, 10, 20 and 40 μg) for 24 h in the presence or absence of IL-1β. The viability of NP cells was detected using Cell Counting Kit-8 (CCK-8) assays. (E) The viability of IL-1β-stimulated NP cells treated with Exo-HO-1 (20 μg) for different times (0, 12, 14, 48 and 72 h) was determined by CCK-8 assays. ***P<0.001. IL, interleukin; Exo, exosomes; HO-1, heme oxygenase 1; NP, nucleus pulposus.

stimulation caused NP cells to senesce and arrest in the G_0/G_1 phase, although this effect was substantially attenuated upon treatment with Exo-HO-1 but not with Exo (Fig. 5B). Together, these outcomes indicated that IL-1β-induced NP cell senescence could be alleviated by Exo-HO-1.

Exo-HO-1 suppresses the NF-κB signaling in IL-1β-stimulated NP cells. Considering that NF-κB exerts a vital action in the progression of IVDD (38), the present study further analyzed whether Exo-HO-1 works by mediating the NF-κB signaling. IL-1β promoted the phosphorylation of p65 protein, although Exo-HO-1 and Exo decreased the phosphorylation of p65 protein and Exo-HO-1 had a stronger effect than Exo (Fig. 6). NF-κB p65 was predominantly distributed in the cytoplasm of control cells, whereas IL-1β stimulation boosted the translocation of NF-κB p65 from the cytoplasm to the nucleus. However, Exo and Exo-HO-1 suppressed the nuclear translocation of NF-κB p65. Activation of the NF-κB signaling mediated by IL-1β stimulation was restrained in NP cells after Exo-HO-1 treatment.

Discussion

Exosomes applied alone or loaded with specific genes or drugs are important tools for exchanging information between IVDD (39). Some studies have reported that BMSC-derived exosomes ameliorate IVDD (40) and a few studies have reported on the function of genetically modified BMSC-derived exosomes in IVDD. BMSC-derived exosomes and HO-1 have both been demonstrated to exert protective effects against IVDD progression, but the innovation of the present study was to reveal that BMSC-derived exosomes modified with HO-1 attenuated IL-1β-induced NP cell apoptosis and senescence, suggesting that HO-1-modified BMSC-derived exosomes may be a promising strategy for IVDD treatment.

The inflammatory response is a key pathological mechanism in the development of IVDD and the overexpression of pro-inflammatory cytokines can disrupt extracellular matrix homeostasis in IVD and enable it to maintain degenerative and catabolic states (41). IL-1β, as an important pro-inflammatory factor involved in cell differentiation and apoptosis through the NF-κB signaling pathway, is frequently used to induce degeneration of NPCs for establishing IVDD cell models *in vitro* (42,43). The present study observed that IL-1β (10 and 20 ng/ml) stimulation markedly drove NP cell apoptosis. The apoptosis of NP cells was shifted to a later stage when the concentration of IL-1β reached 20 ng/ml or 10 ng/ml. IL-1β was treated for 48 h, so NP cells with were stimulated 10 ng/ml of IL-1β for 24 h to induce IVDD cell models *in vitro*.

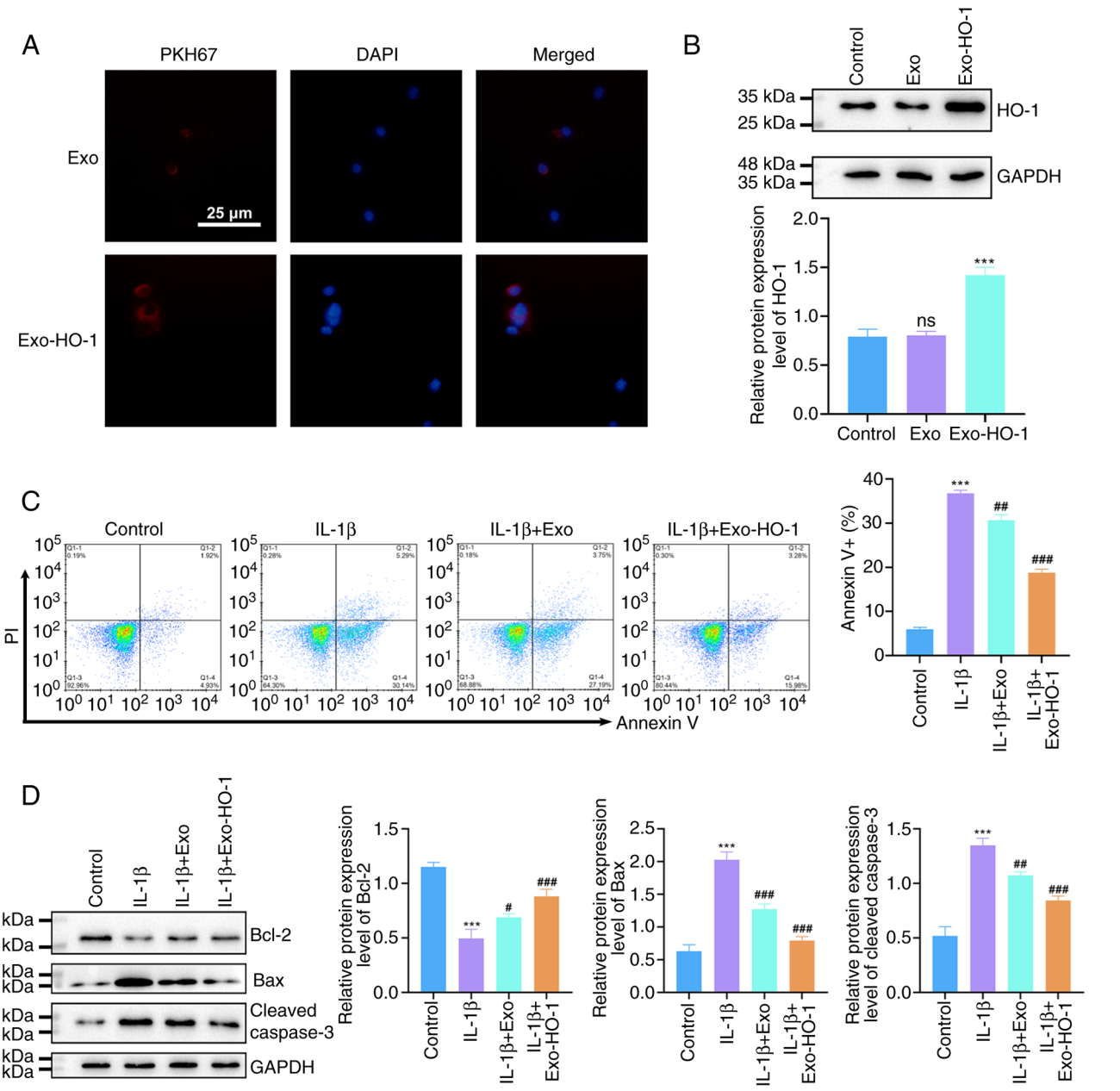

Figure 4. Exo-HO-1 ameliorated IL-1β-induced apoptosis in NP cells. (A) Internalization of PKH26-labeled Exo or Exo-HO-1 by NP cells was examined by confocal microscopy after 24 h of co-incubation (scale bar,25 μm). (B) Protein levels of HO-1 in NP cells co-cultured with phosphate-buffered saline, Exo, or Exo-HO-1 were detected by western blotting. (C) Flow cytometry analysis of the apoptosis of NP cells in different groups (control, IL-1β, IL-1β + Exo and IL-1β + Exo-HO-1). (D) Western blotting detected apoptosis-associated proteins Bcl-2, Bax and Cleaved caspase 3 in NP cells with different treatments. ns: not significant. ***P<0.001 vs. control; $^{\#}$P<0.05, $^{\#\#}$P<0.01 and $^{\#\#\#}$P<0.001 vs. IL-1β; ns, not significant. Exo, exosomes; HO-1, heme oxygenase 1; IL, interleukin; NP, nucleus pulposus.

Currently, BMSC-derived exosomes have become the focus as a potential alternative to BMSCs in cell therapy including IVDD. Hu *et al* have reported that BMSC-derived exosomes repress compression-mediated oxidative stress in NP cells, thus alleviating apoptosis (44). BMSC-derived exosomes modulate the Keap1/Nrf2 axis, thereby restoring the antioxidant response in degenerative NP cells (40). HO-1, which exhibits anti-inflammatory, antioxidant and anti-apoptotic properties, is a protein downstream of Nrf2 (25). Furthermore, cyanidin-3-glucoside and dimethyl fumarate weaken the dysfunction of NP cells via the Nrf2/HO-1 pathway during IVDD (24,45). Another report has indicated that HO-1 expression is low in IVDD samples (46) and HO-1 overexpression can protect NP cell apoptosis under IL-1β stimulation (46,47). However, the effects of BMSC-derived exosomes loaded with HO-1 on NP cell apoptosis and senescence are unclear.

The present study characterized BMSCs by multilineage differentiation and detection of surface marker molecules. Furthermore, exosomes isolated from BMSCs and BMSCs overexpressing HO-1 showed little differences in size and morphology. In addition, Exo-HO-1 treatment at a low dose (10 μg) could improve the viability of NP cells under IL-1β stimulation. Incubation of IL-1β-induced NP cells

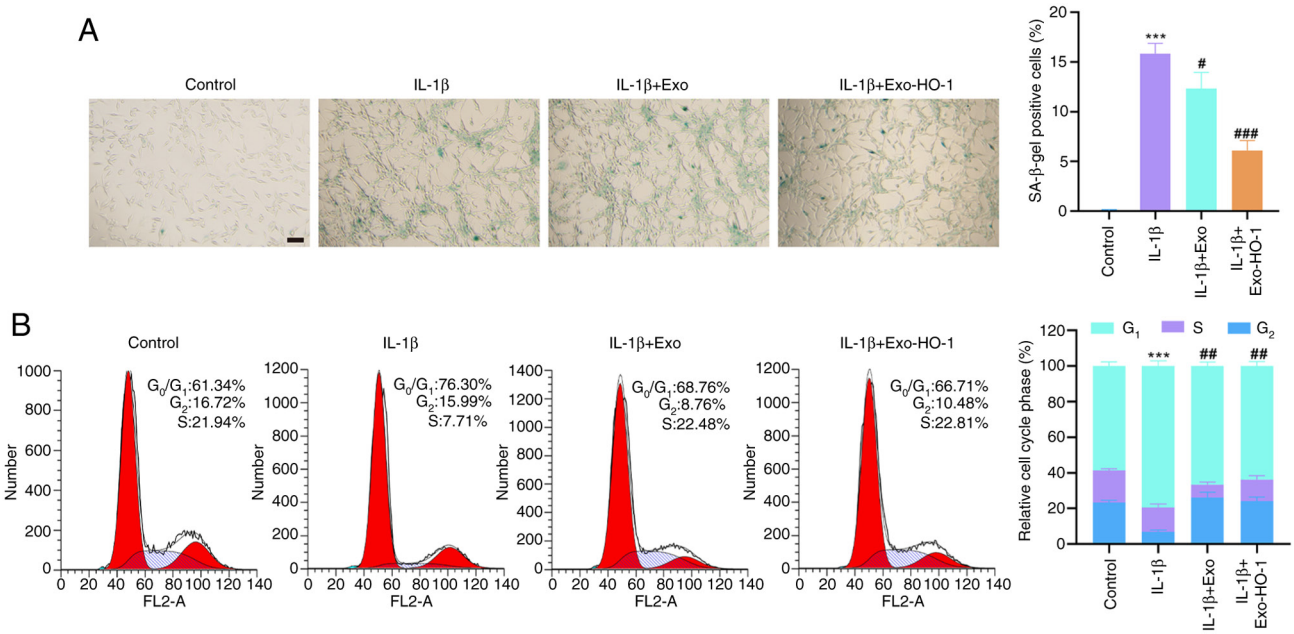

Figure 5. Exo-HO-1 protected NP cells against IL-1β-induced senescence. (A) SA-β-gel staining detected the expression of β-gel in NP cells with different treatments (control, IL-1β, IL-1β + Exo and IL-1β + Exo-HO-1). (B) Flow cytometry analysis of cell cycle progression in NP cells from different groups. ***P<0.001 vs. control; #P<0.05, ##P<0.01 and ###P<0.001 vs. IL-1β. Exo, exosomes; HO-1, heme oxygenase 1; NP, nucleus pulposus; IL, interleukin.

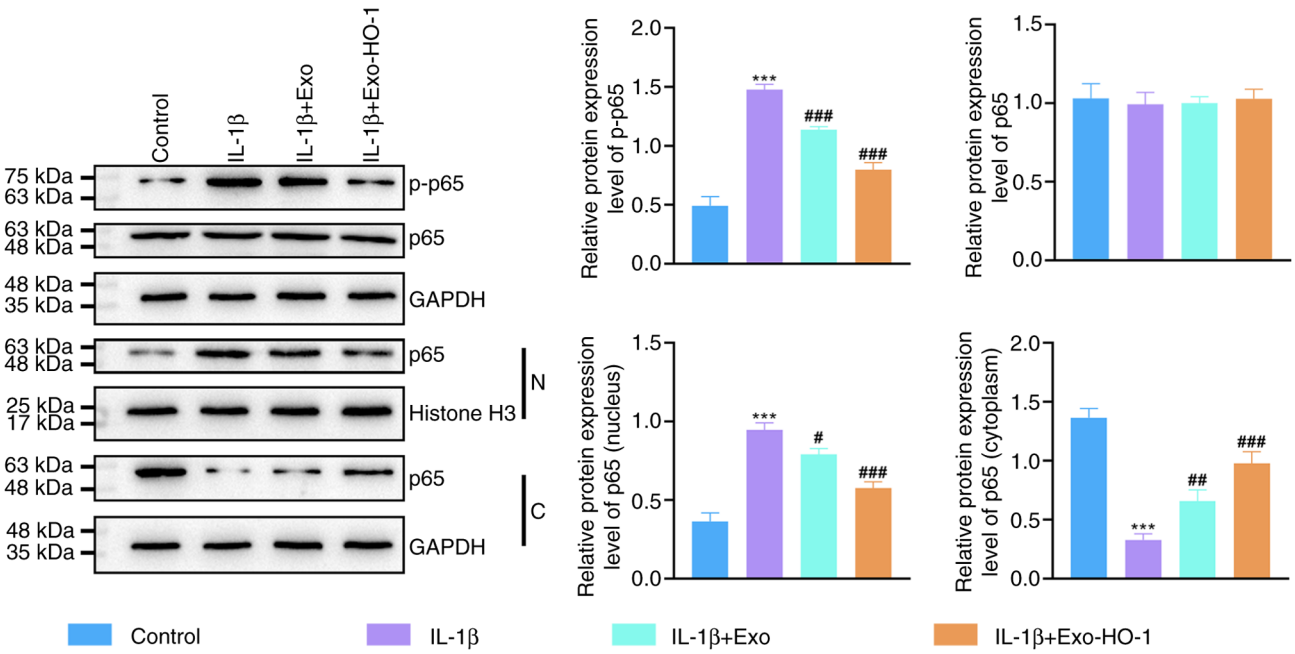

Figure 6. Activation of the NF-κB signalling in NP cells induced by IL-1β was repressed after Exo-HO-1 treatment. Western blotting was performed to detect p-p65 and/or p65 protein levels in NP cells with different treatments (control, IL-1β, IL-1β + Exo and IL-1β + Exo-HO-1) as well as in the nuclear (N) and cytoplasmic (C) fractions of the cells. Histone H3 was used as an internal reference for the nucleus. ***P<0.001 vs. control; #P<0.05, ##P<0.01 and ###P<0.001 vs. IL-1β. NP, nucleus pulposus; IL, interleukin; Exo, exosomes; HO-1, heme oxygenase 1; p-phosphorylated.

with Exo-HO-1 for ≥24 h clearly increased their activity, so IL-1β-stimulated NP cells were treated with Exo-HO-1 (10 μg) for 24 h and used for function analysis. Functionally, Exo-HO-1 treatment markedly reduced IL-1β-induced NP cell apoptosis, accompanied with a simultaneous alteration in Bcl-2, cleaved caspase 3 and Bax levels. In addition, both Exo and Exo-HO-1 treatment weakened IL-1β-prompted senescence in NP cells and Exo-HO-1 had a stronger effect than Exo. These results highlighted the important role of Exo-HO-1 in apoptosis and senescence of NP cells.

NF-κB signaling is a target for pro-inflammatory factors, such as tumor necrosis factor-alpha, IL-1β and IL-8, triggering a cytokine storm and playing a central role in the inflammatory response (48). NF-κB proteins are inactivated in the cytoplasm by binding to the repressor protein IkB to form a trimeric complex (49). However, the NF-κB dimer exposes

nuclear localization sequences and rapidly passes from the cytoplasm into the nucleus when upstream signaling factors bind to receptors on the surface of the cell membrane, followed by binding to specific sequences on nuclear DNA to promote the transcription of relevant genes (49). The NF-κB signaling pathway is closely related to the process of IVDD and blocking the NF-κB signaling pathway markedly delays IVDD (50,51). In the present study, Exo-HO-1 and Exo treatment decreased the phosphorylation of the p65 protein in IL-1β-induced NP cells and Exo-HO-1 had a stronger effect than Exo. However, Exo and Exo-HO-1 repressed the nuclear translocation of NF-κB p65, suggesting that IL-1β-urged activation of the NF-κB signaling was restrained in NP cells after Exo-HO-1 treatment. Unfortunately, the present study did not use animal models of disc degeneration to validate the therapeutic effect of Exos or Exo-HO-1 on disc recovery, which will be the direction of future research.

In conclusion, Exo-HO-1 delivered HO-1 to IL-Iβ-induced NP cells and repressed the nuclear translocation of p65, resulting in ameliorating NP cell apoptosis and senescence. The protective effect of Exo-HO-1 may depend on HO-1. Therefore, the use of BMSCs-derived exosomes as HO-1 carriers may be a promising approach for IVDD treatment. The present study offers a promising therapeutic strategy for IVDD.

Acknowledgements

Not applicable.

Funding

The present study was supported by the National Natural Science Foundation of China (grant no. 82072496).

Availability of data and materials

The data generated in the present study may be requested from the corresponding author.

Authors' contributions

HZ, DZ and XZM conceived the study and designed the experiments. HW, YLL, WYD and GPF contributed to data collection, performed data analysis and interpreted the results. HZ and DZ wrote the manuscript. XZM contributed to critical revision of this article. HW, YLL, WYD and GPF confirm the authenticity of all the raw data. All authors have read and approved the final version of the manuscript.

Ethics approval and consent to participate

Not applicable.

Patient consent for publication

Not applicable.

Competing interests

The authors declare that they have no competing interests.

References

1. Mohd Isa IL, Teoh SL, Mohd Nor NH and Mokhtar SA: Discogenic low back Pain: Anatomy, pathophysiology and treatments of intervertebral disc degeneration. Int J Mol Sci 24: 208, 2022.
2. The Lancet Rheumatology: The global epidemic of low back pain. Lancet Rheumatol 5: e305, 2023.
3. Safiri S, Kolahi AA, Cross M, Hill C, Smith E, Carson-Chahhoud K, Mansournia MA, Almasi-Hashiani A, Ashrafi-Asgarabad A, Kaufman J, *et al*: Prevalence, deaths, and Disability-adjusted life years due to musculoskeletal disorders for 195 countries and territories 1990-2017. Arthritis Rheumatol 73: 702-714, 2021.
4. Ohnishi T, Iwasaki N and Sudo H: Causes of and molecular targets for the treatment of intervertebral disc degeneration: A review. Cells 11: 394, 2022.
5. Zehra U, Tryfonidou M, Iatridis JC, Illien-Jünger S, Mwale F and Samartzis D: Mechanisms and clinical implications of intervertebral disc calcification. Nat Rev Rheumatol 18: 352-362, 2022.
6. Mohd Isa IL, Mokhtar SA, Abbah SA, Fauzi MB, Devitt A and Pandit A: Intervertebral disc degeneration: Biomaterials and tissue engineering strategies toward precision medicine. Adv Healthc Mater 11: e2102530, 2022.
7. Munda M and Velnar T: Stem cell therapy for degenerative disc disease: Bridging the gap between preclinical promise and clinical potential. Biomol Biomed 24: 210-218, 2024.
8. Hajiesmailpoor A, Mohamadi O, Farzanegan G, Emami P and Ghorbani M: Overview of stem cell therapy in intervertebral disc disease: Clinical perspective. Curr Stem Cell Res Ther 18: 595-607, 2023.
9. Yuan X, Yuan W, Ding L, Shi M, Luo L, Wan Y, Oh J, Zhou Y, Bian L and Deng DY: Cell-adaptable dynamic hydrogel reinforced with stem cells improves the functional repair of spinal cord injury by alleviating neuroinflammation. Biomaterials 279: 121190, 2021.
10. Kalluri R and LeBleu VS: The biology, function, and biomedical applications of exosomes. Science 367: eaau6977, 2020.
11. Xiao Q, Zhao Z, Teng Y, Wu L, Wang J, Xu H, Chen S and Zhou Q: BMSC-Derived exosomes alleviate intervertebral disc degeneration by modulating AKT/mTOR-Mediated autophagy of nucleus pulposus cells. Stem Cells Int 2022: 9896444, 2022.
12. Li W, Xu Y and Chen W: Bone mesenchymal stem cells deliver exogenous lncRNA CAHM via exosomes to regulate macrophage polarization and ameliorate intervertebral disc degeneration. Exp Cell Res 421: 113408, 2022.
13. Bhujel B, Shin HE, Choi DJ and Han I: Mesenchymal stem Cell-derived exosomes and intervertebral disc regeneration: Review. Int J Mol Sci 23: 7306, 2022.
14. DiStefano TJ, Vaso K, Danias G, Chionuma HN, Weiser JR and Iatridis JC: Extracellular vesicles as an emerging treatment option for intervertebral disc degeneration: Therapeutic potential, translational pathways, and regulatory considerations. Adv Healthc Mater 11: 2100596, 2022.
15. Jiang Y, Hu J, Cui C, Peng Z, Yang S, Lei J, Li B, Yang X, Qin J, Yin M, *et al*: Netrin1-enriched exosomes from genetically modified ADSCs as a novel treatment for diabetic limb ischemia. Adv Healthc Mater 14: e2403521, 2025.
16. Xiao B, Zhu Y, Liu M, Chen M, Huang C, Xu D, Wang F, Sun S, Huang J, Sun N, *et al*: Correction: Mir-340-3p-modified bone marrow mesenchymal stem cell-derived exosomes inhibit ferroptosis through METTL3-mediated m6A modification of HMOX1 to promote recovery of injured rat uterus. Stem Cell Res Ther 15: 357, 2024.
17. Gozzelino R, Jeney V and Soares MP: Mechanisms of cell protection by heme oxygenase-1. Annu Rev Pharmacol Toxicol 50: 323-354, 2010.
18. Zhou X, Zhang Y, Hou M, Liu H, Yang H, Chen X, Liu T, He F and Zhu X: Melatonin prevents cartilage degradation in Early-stage osteoarthritis through activation of miR-146a/NRF2/HO-1 axis. J Bone Miner Res 37: 1056-1072, 2022.
19. Feng X, Wang S, Sun Z, Dong H, Yu H, Huang M and Gao X: Ferroptosis enhanced diabetic renal tubular injury via HIF-1α/HO-1 pathway in db/db mice. Front Endocrinol (Lausanne) 12: 626390, 2021.
20. Wei R, Zhao Y, Wang J, Yang X, Li S, Wang Y, Yang X, Fei J, Hao X, Zhao Y, *et al*: Tagitinin C induces ferroptosis through PERK-Nrf2-HO-1 signaling pathway in colorectal cancer cells. Int J Biol Sci 17: 2703-2717, 2021.

21. Liu J, Huang J, Zhang Z, Zhang R, Sun Q, Zhang Z, Liu Y and Ma B: Mesenchymal stem Cell-derived exosomes ameliorate delayed neurocognitive recovery in aged mice by inhibiting hippocampus ferroptosis via activating SIRT1/Nrf2/HO-1 signaling pathway. Oxid Med Cell Longev 2022: 3593294, 2022.
22. Luo Y, He YZ, Wang YF, Xu YX and Yang L: Adipose-derived mesenchymal stem cell exosomes ameliorate spinal cord injury in rats by activating the Nrf2/HO-1 pathway and regulating microglial polarization. Folia Neuropathol 61: 326-335, 2023.
23. Kao YH, Chang CY, Lin YC, Chen PH, Lee PH, Chang HR, Chang WY, Chang YC, Wun SF and Sun CK: Mesenchymal stem Cell-derived exosomes mitigate acute murine liver injury via Ets-1 and heme oxygenase-1 Up-regulation. Curr Stem Cell Res Ther 19: 906-918, 2023.
24. Bai X, Lian Y, Hu C, Yang S, Pei B, Yao M, Zhu X, Shang L and Li Z: Cyanidin-3-glucoside protects against high glucose-induced injury in human nucleus pulposus cells by regulating the Nrf2/HO-1 signaling. J Appl Toxicol 42: 1137-1145, 2022.
25. Zhang CY, Hu XC, Zhang GZ, Liu MQ, Chen HW and Kang XW: Role of Nrf2 and HO-1 in intervertebral disc degeneration. Connect Tissue Res 63: 559-576, 2022.
26. Lei H, He M, He X, Li G, Wang Y, Gao Y, Yan G, Wang Q, Li T, Liu G, *et al*: METTL3 induces bone marrow mesenchymal stem cells osteogenic differentiation and migration through facilitating M1 macrophage differentiation. Am J Transl Res 13: 4376-4388, 2021.
27. Wang Y, Hang K, Ying L, Wu J, Wu X, Zhang W, Li L, Wang Z, Bai J and Gao X: LAMP2A regulates the balance of mesenchymal stem cell adipo-osteogenesis via the Wnt/β-catenin/GSK3β signaling pathway. J Mol Med (Berl) 101: 783-799, 2023.
28. Zhu Q, Fu Y, Cui CP, Ding Y, Deng Z, Ning C, Hu F, Qiu C, Yu B, Zhou X, *et al*: OTUB1 promotes osteoblastic bone formation through stabilizing FGFR2. Signal Transduct Target Ther 8: 142, 2023.
29. Zhao J, Ding Y, He R, Huang K, Liu L, Jiang C, Liu Z, Wang Y, Yan X, Cao F, *et al*: Dose-effect relationship and molecular mechanism by which BMSC-derived exosomes promote peripheral nerve regeneration after crush injury. Stem Cell Res Ther 11: 360, 2020.
30. Song L, Tang S, Han X, Jiang Z, Dong L, Liu C, Liang X, Dong J, Qiu C, Wang Y, *et al*: KIBRA controls exosome secretion via inhibiting the proteasomal degradation of Rab27a. Nat Commun 10: 1639, 2019.
31. Tang YT, Huang YY, Zheng L, Qin SH, Xu XP, An TX, Xu Y, Wu YS, Hu XM, Ping BH, *et al*: Comparison of isolation methods of exosomes and exosomal RNA from cell culture medium and serum. Int J Mol Med 40: 834-844, 2017.
32. Wang Q, Wang H, Zhao X, Han C, Liu C, Li Z, Du T, Sui Y, Zhang X, Zhang J, *et al*: Transcriptome sequencing of circular RNA reveals the involvement of hsa-SCMH1_0001 in the pathogenesis of Parkinson's disease. CNS Neurosci Ther 30: e14435, 2024.
33. Tian Y, Yuan W, Fujita N, Wang J, Wang H, Shapiro IM and Risbud MV: Inflammatory cytokines associated with degenerative disc disease control aggrecanase-1 (ADAMTS-4) expression in nucleus pulposus cells through MAPK and NF-κB. Am J Pathol 182: 2310-2321, 2013.
34. Shi C, Wu H, Du D, Im HJ, Zhang Y, Hu B, Chen H, Wang X, Liu Y, Cao P, *et al*: Nicotinamide phosphoribosyltransferase inhibitor APO866 prevents IL-1β-Induced human nucleus pulposus cell degeneration via autophagy. Cell Physiol Biochem 49: 2463-2482, 2018.
35. Li M, Li R, Yang S, Yang D, Gao X, Sun J, Ding W and Ma L: Exosomes derived from bone marrow mesenchymal stem cells prevent acidic pH-induced damage in human nucleus pulposus cells. Med Sci Monit 26: e922928, 2020.
36. Zhang C, Lu Z, Lyu C, Zhang S and Wang D: Andrographolide inhibits static mechanical Pressure-Induced intervertebral disc degeneration via the MAPK/Nrf2/HO-1 pathway. Drug Des Devel Ther 17: 535-550, 2023.
37. Yao B, Cai Y, Wan L, Deng J, Zhao L, Wang W and Han Z: BACH1 promotes intervertebral disc degeneration by regulating HMOX1/GPX4 to mediate oxidative stress, ferroptosis, and lipid metabolism in nucleus pulposus cells. J Gene Med 25: e3488, 2023.
38. Zhang GZ, Liu MQ, Chen HW, Wu ZL, Gao YC, Ma ZJ, He XG and Kang XW: NF-κB signalling pathways in nucleus pulposus cell function and intervertebral disc degeneration. Cell Prolif 54: e13057, 2021.
39. Hu YC, Zhang XB, Lin MQ, Zhou HY, Cong MX, Chen XY, Zhang RH, Yu DC, Gao XD and Guo TW: Nanoscale treatment of intervertebral disc degeneration: mesenchymal stem cell exosome transplantation. Curr Stem Cell Res Ther 18: 163-173, 2023.
40. Xu G, Lu X, Liu S, Zhang Y, Xu S, Ma X, Xia X, Lu F, Zou F, Wang H, *et al*: MSC-Derived exosomes ameliorate intervertebral disc degeneration by regulating the Keap1/Nrf2 axis. Stem Cell Rev Rep 19: 2465-2480, 2023.
41. Lee S, Moon CS, Sul D, Lee J, Bae M, Hong Y, Lee M, Choi S, Derby R, Kim BJ, *et al*: Comparison of growth factor and cytokine expression in patients with degenerated disc disease and herniated nucleus pulposus. Clin Biochem 42: 1504-1511, 2009.
42. Liu H, Liu H, Meng Z and Zhang W: Mechanism of KMT2D-mediated epigenetic modification in IL-1β-induced nucleus pulposus cell degeneration. Histol Histopathol 18813, 2024.
43. Xia J, Jia D and Wu J: Protective effects of alpinetin against interleukin-1β-exposed nucleus pulposus cells: Involvement of the TLR4/MyD88 pathway in a cellular model of intervertebral disc degeneration. Toxicol Appl Pharmacol 492: 117110, 2024.
44. Hu Y, Tao R, Wang L, Chen L, Lin Z, Panayi AC, Xue H, Li H, Xiong L and Liu G: Exosomes derived from bone mesenchymal stem cells alleviate Compression-Induced nucleus pulposus cell apoptosis by inhibiting oxidative stress. Oxid Med Cell Longev 2021: 2310025, 2021.
45. Wang R, Luo D, Li Z and Han H: Dimethyl fumarate ameliorates nucleus pulposus cell dysfunction through activating the Nrf2/HO-1 pathway in intervertebral disc degeneration. Comput Math Methods Med 2021: 6021763, 2021.
46. Zhu C, Jiang W, Cheng Q, Hu Z and Hao J: Hemeoxygenase-1 suppresses IL-1β-induced apoptosis through the NF-κB pathway in human degenerative nucleus pulposus cells. Cell Physiol Biochem 46: 644-653, 2018.
47. Zou L, Lei H, Shen J, Liu X, Zhang X, Wu L, Hao J, Jiang W and Hu Z: HO-1 induced autophagy protects against IL-1 β-mediated apoptosis in human nucleus pulposus cells by inhibiting NF-κB. Aging (Albany NY) 12: 2440-2452, 2020.
48. Lawrence T: The nuclear factor NF-kappaB pathway in inflammation. Cold Spring Harb Perspect Biol 1: a001651, 2009.
49. Bacher S, Meier-Soelch J, Kracht M and Schmitz ML: Regulation of transcription factor NF-κB in its natural habitat: The nucleus. Cells 10: 753, 2021.
50. Liao Y, Tan RZ, Li JC, Liu TT, Zhong X, Yan Y, Yang JK, Lin X, Fan JM and Wang L: Isoliquiritigenin attenuates UUO-Induced renal inflammation and fibrosis by inhibiting Mincle/Syk/NF-Kappa B signaling pathway. Drug Des Devel Ther 14: 1455-1468, 2020.
51. Zhongyi S, Sai Z, Chao L and Jiwei T: Effects of nuclear factor kappa B signaling pathway in human intervertebral disc degeneration. Spine (Phila Pa 1976) 40: 224-32, 2015.